ACADEMIC PRESS

Available online at www.sciencedirect.com

SCIENCE DIRECT®

Journal of Sound and Vibration 265 (2003) 1–22

JOURNAL OF SOUND AND VIBRATION

www.elsevier.com/locate/jsvi

Crack detection in beams using changes in frequencies and amplitudes of frequency response functions

G.M. Owolabi, A.S.J. Swamidas*, R. Seshadri

Faculty of Engineering and Applied Sciences, Memorial University of Newfoundland, St John's, Newfoundland, Canada A1B 3X5

Received 24 May 2001; accepted 20 August 2002

Abstract

In recent years, significant efforts have been devoted to developing non-destructive techniques for damage identification in structures. The work reported in this paper is part of an ongoing research on the experimental investigations of the effects of cracks and damages on the integrity of structures, with a view to detect, quantify, and determine their extents and locations. Two sets of aluminum beams were used for this experimental study. Each set consisted of seven beams, the first set had fixed ends, and the second set was simply supported. Cracks were initiated at seven different locations from one end to the other end (along the length of the beam) for each set, with crack depth ratios ranging from $0.1d$ to $0.7d$ (d is the beam depth) in steps of 0.1, at each crack location. Measurements of the acceleration frequency responses at seven different points on each beam model were taken using a dual channel frequency analyzer.

The damage detection schemes used in this study depended on the measured changes in the first three natural frequencies and the corresponding amplitudes of the measured acceleration frequency response functions.

1. Introduction

A large number of studies have been carried out on conventional (dye penetrant, magnetic particle induction, ultrasonic, etc.) and modern approaches to non-destructive testing and evaluation. The conventional methods have been well developed, implemented in widely marketed equipment, and accepted by industry and regulatory agencies as practically applicable non-destructive evaluation (NDE) methods. The modern NDE methods are still under development, implemented in a limited manner in some equipment and not fully accepted by the industry and

*Corresponding author. Tel.: +709-737-7983; fax: 709-737-4042.
E-mail address: swamidas@engr.mun.ca (A.S.J. Swamidas).

0022-460X/03/$ - see front matter
doi:10.1016/S0022-460X(02)01264-6

regulatory agencies as practicably applicable NDE methods. One of these modern methods is the vibration-based inspection methodology.

A comprehensive survey of available literature on damaged structures was carried out by Richardson [1], to determine the current state of the crack detection technology. The paper discussed the various methods used for structural integrity monitoring of nuclear power plants, large civil engineering structures, rotating machinery, etc. A more comprehensive survey was presented later by Doebling et al. [2]. This survey reviewed the numerous technical literature available on detection, sizing and location of structural damage via vibration-based testing. It categorized the various methods available for crack detection according to the measured data and analysis techniques.

An earlier study carried out by Cawley and Adams [3] noted that the stress distribution through a vibrating structure was non-uniform and was different for each natural frequency (mode). The authors stated that any localized damage would affect each mode differently, depending on the particular location of the damage. Consequently, the measurement of the natural frequencies of a structure at two or more stages of its lifetime offered the possibility of locating damage in any structure and of determining the severity of the damage. The numerical results obtained in this study, using finite element method, were verified by experimental results. An alternative approach referred to as sensitivity (perturbation) analysis was also used in the paper. In this approach, the sensitivities of natural frequencies of a system to small changes in stiffness were calculated from the mode shapes of the undamaged structure. The damage location was calculated using the loci for several pairs of modes, i.e., locations at which the ratio of the experimentally determined changes equaled the theoretical ratio. These two approaches produced excellent agreement.

Dynamically loaded beams with cross-sectional cracks have been investigated in a number of studies. Silva and Gomes [4] used experimental modal analysis to measure the natural frequencies of slotted and fatigue-cracked beams. Ju and Mimovich [5] were able to model cracks in a cantilever beam using a fracture hinge. They tested aluminum beams with a cross-sectional area of $9.5\,\text{mm} \times 63.5\,\text{mm}$, and of length 457 mm, to verify their numerical results. Fox [6] conducted modal tests on a beam with saw cuts. He used soft springs to simulate the boundary conditions during the tests. He also carried out a finite element analysis of the test specimen. Damage was estimated using the relative changes in mode shapes whose frequencies shifted because of the damage. Choudhury and Ramirez [7] performed modal tests on both reinforced and plain concrete beams. They made quantitative measurement of the changes in resonant frequencies and power spectral densities of displacements resulting from simulated damage, changes in mechanical properties, and changes in the applied load. Prime and Shevitz [8] carried out experimental modal testing and analysis on a polycarbonate cantilever beam having an opening and closing crack in the interior of the beam, running parallel to the top and bottom surfaces. The beam was tested by alternate pulling and releasing. Its non-linear response was then monitored and the results explained through the use of a number of techniques.

Stubbs [9] used an energy-based theoretical approach and experimental validation to detect the influence of defects in a structure. In an earlier study, Chondros and Dimarogonas [10] had investigated the effects of cracks in welded joints using fracture mechanics concepts. The change in the bending stiffness of a beam due to a crack was measured and used in the mathematical model. They developed a frequency spectral method to identify cracks in various structures. Chondros and Dimarogonas [11,12] used energy method and a continuous cracked beam theory

for analyzing the transverse vibration of cracked beams. Using the earlier concepts developed by Christides and Barr [13], this theory used analytical expressions obtained for the stress field from basic equilibrium formulations and from well-established fracture mechanics equations for cracked structures. The paper presented results of the lowest natural frequencies of flexural vibration (obtained from two different models), of a cantilever beam with a single edge crack; it also compared the analytical results with values obtained from tests. It was stated that the method could be extended to other modes of vibration, geometries and boundary conditions as well as to coupled lateral and torsional vibration problems.

Perchard and Swamidas [14] carried out frequency measurements on narrow cantilever plates (or wide beams) with sawed notches. Results obtained experimentally, as well as numerically (using finite element methods), showed that the crack could be detected mainly through the changes in natural frequencies for a number of modes. In addition the slopes, along the length of the beam and around the discontinuous notches, were obtained numerically for a number of lower modes; they were subsequently used for crack detection. Budipriyanto and Swamidas [15] and Chen and Swamidas [16] investigated the influence of cracks on plates and welded T-joints (in air and water). They incorporated experimental testing, finite element analysis, system identification and model updating procedures for developing a methodology for detecting and quantifying growing surface cracks in plated T-joints. In addition, Chen and Swamidas [16] also obtained detailed two-dimensional crack growth profiles of plated T-joints, using vibration measurements. They stated that surface strain measurements and curvature changes that occur around cracks would be the best indicators for crack detection and identification.

In the present paper, an attempt has been made to detect the presence of a crack in beams, and determine its location and size, based on experimental modal analysis results. The results were obtained from measurements of dynamic responses of cracked beams. Changes in natural frequencies and frequency response function (FRF) amplitudes as a function of crack depths and locations were used in the crack detection methodology.

2. Basic equation

The basic linear differential equation of motion, of a multi-degree-of-freedom (m.d.o.f.) structure, is given by

$$[M]\{\ddot{x}\} + [C]\{\dot{x}\} + [K]\{x\} = \{F(t)\}, \tag{1}$$

where $[M]$ is the mass matrix, $[C]$ the damping matrix, $[K]$ the stiffness matrix, $\{x(t)\}$ the displacement vector, $\{\dot{x}(t)\}$ the velocity vector, and $\{\ddot{x}(t)\}$ the acceleration vector.

The above equation balances the structure's internal forces, which are a combination of mass (inertial), damping (dissipative), and stiffness (elastic restoring) terms (referred to the spatial model) with the externally applied forces. Defects existing in a structure cause a change in its stiffness, and could also affect its mass distribution, and damping properties. Consequently, there would also be a change in the dynamic response of the structure. In addition to Eq. (1) shown above, the linear dynamics could also be represented by other equivalent expressions such as the FRF, modal parameters or the impulse response function. Therefore, if the acquired FRF, modal parameters or the impulse response of the structure undergoes a change, there will be a

corresponding change in its mass, damping, and/or stiffness properties. This is the basis for using modal analysis in damage detection.

3. Experimental set-up and procedures

3.1. Experimental model description

Two sets of aluminum beams were used for this experimental investigation. Each set consisted of seven beam models; the first set had fixed ends, while the second set had simply supported ends. Each beam model was made of an aluminum bar of cross-sectional area 25.4 mm × 25.4 mm with a length of 650 mm. It had the following material properties: Young's modulus $E = 70\,\text{GPa}$, density $\rho = 2.696\,\text{gm/cm}^3$, the Poisson ratio $v = 0.35$.

3.2. Experimental procedures

The fixed–fixed beam model was clamped at each end, between two thick square steel plates, supported over a short and stiff steel H-section column. The exciter was suspended using a slotted square flat plate; the slotted square plate was fixed to the bottom of the top beam (of the steel frame) by four threaded rods. This made possible the adjustment of the position of the exciter whenever a model was to be attached.

The first three natural frequencies of the uncracked beam were measured. Then, cracks were generated to the desired depth using a thin saw cut (around 0.4 mm thick); the crack always remained open during dynamic testing. For each set, seven beam models were tested with cracks at seven different locations, starting from a location near to one of the clamped or simply supported ends. The crack depth varied from $0.1d$ to $0.7d$ (d is the depth of the beam = 25.4 mm) with an increment of $0.1d$ at each crack position.

Each model was excited by a fast sine sweep signal produced by the function generator, which was then amplified, and used to drive the exciter, which eventually transmitted the force to the beam model through the load cell. This served as the input to the system. It is to be noted that the model was excited at a point, which was a few millimeters away from the center of the model. This was done to avoid exciting the beam at a nodal point (of a mode), since the beam would not respond for that mode at that point.

The dynamic responses of the beam model were measured by using seven light accelerometers placed at different points on the model as indicated in Fig. 1. The response measurements were acquired, one at a time, using the dual channel signal analyzer. Prior to the response computation by the analyzer, the monitored signals were passed through a filter to eliminate the extraneous noise as indicated by Allemang [17]. The measured frequency responses, acquired using the signal analyzer, were given a 100 ensemble averaging before transferring them through GPIB to the PC on which a Structural Testing, Analysis, and Reporting (STAR) software package was installed for data analysis.

A total of three modes were identified in four frequency ranges (for beams with fixed ends), and three frequency ranges (for beams with simply supported ends), respectively. It was observed that an unexpected resonant frequency was generated by the vibration of the thick floor plate, and its

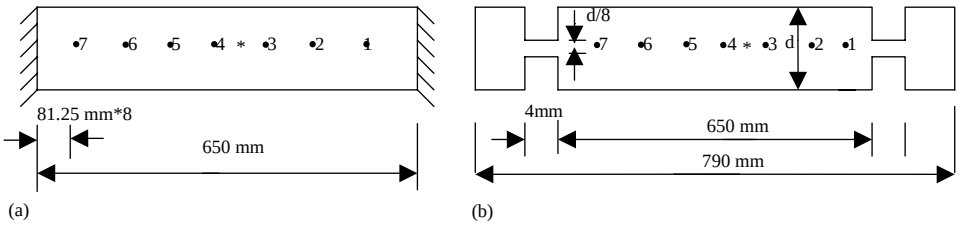

Fig. 1. Locations of accelerometers: (a) fixed–fixed beam, (b) simply supported beam (*, point of excitation; •, accelerometer point).

support. These were identified using an eighth accelerometer placed on the floor/support and monitoring the responses to see whether the frequency response was due to the floor/support vibration or due to actual structural vibration (in this case, the tested beams).

4. Results and discussions

4.1. Results

The FRFs obtained were curve-fitted using the STAR Structural Analysis software package. The experimental data from the curve-fitted results were tabulated, and plotted (in a three-dimensional plot) in the form of frequency ratio (ω_c/ω) (ratio of the natural frequency of the cracked beam to that of the uncracked beam) versus the crack depth ratio (a/h) (the ratio of the depth of a crack (a) to the thickness of the beam (h)) for various crack location ratios (c/l) (ratio of the location of the crack to the length of the beam). The results that could not be obtained due to experimental errors were regarded as non-available (NA). Tables 1–6 show the variation of the frequency ratio as a function of the crack depth and crack location for beams with fixed and simply supported ends.

4.2. Changes in natural frequencies

Figs. 2 and 3 show the plots of the variations of the first three frequency ratios as a function of crack depth ratios for some of the crack positions considered for each set of boundary conditions (seven locations were considered for each set of boundary conditions). Figs. 4 and 5 illustrate the variations of the first two natural frequencies as a function of crack location for fixed-end and simply supported beams when the crack depth ratio is 0.2, respectively. Note that due to insufficient data, the complete variation of the third natural frequency as a function of crack location could not be plotted accurately.

From the experimental results and plots, the following observations were made for all the cases considered.

(1) For all the cases considered, the fundamental natural frequency was least affected when the crack was located at a position where the ratio of crack location to length the beam (c/l) was $\frac{1}{16}$. The crack was mostly affected when the crack was located at the center ($c/l = \frac{8}{16}$) for a beam with simply supported ends. In case of a beam with fixed ends, the fundamental natural

Table 1
Fundamental natural frequency ratio (ω_c/ω) as a function of crack location and crack depth for a fixed beam (NA): results not available

a/h	$c/l=\frac{1}{16}$	$c/l=\frac{3}{16}$	$c/l=\frac{5}{16}$	$c/l=\frac{7}{16}$	$c/l=\frac{8}{16}$	$c/l=\frac{11}{16}$	$c/l=\frac{14}{16}$
0	1	1	1	1	1	1	1
0.1	NA	1	1	0.9977	0.9985	1	0.9995
0.2	NA	1	0.9975	0.9900	0.9923	0.9989	0.9980
0.3	NA	1	0.9923	0.9767	0.9746	0.9952	0.9864
0.4	NA	1	0.9825	0.9666	0.9608	0.9815	0.9735
0.5	NA	1	0.9712	0.9222	0.9159	0.9773	0.9602
0.6	NA	1	0.9576	0.8744	0.8726	0.9686	0.9349
0.7	NA	1	0.9523	0.7986	0.8443	0.9318	0.9068

Table 2
Second natural frequency ratio (ω_c/ω) as a function of crack location and crack depth for a fixed beam

a/h	$c/l=\frac{1}{16}$	$c/l=\frac{3}{16}$	$c/l=\frac{5}{16}$	$c/l=\frac{7}{16}$	$c/l=\frac{8}{16}$	$c/l=\frac{11}{16}$	$c/l=\frac{14}{16}$
0	1	1	1	1	1	1	1
0.1	0.9994	0.9982	0.9986	0.9989	1	0.9986	0.9988
0.2	0.9972	0.9938	0.9902	0.9972	1	0.9945	0.9910
0.3	0.9932	0.9875	0.9800	0.9955	1	0.9805	0.9849
0.4	0.9898	0.9864	0.9661	0.9911	1	0.9686	0.9815
0.5	0.9877	0.9596	0.9312	0.9832	1	0.9511	0.9779
0.6	0.9859	0.9498	0.9042	0.9774	1	0.9177	0.9719
0.7	0.9839	0.9284	0.8634	0.9729	1	0.9040	0.9683

Table 3
Third natural frequency ratio (ω_c/ω) as a function of crack location and crack depth for a fixed beam

a/h	$c/l=\frac{1}{16}$	$c/l=\frac{3}{16}$	$c/l=\frac{5}{16}$	$c/l=\frac{7}{16}$	$c/l=\frac{8}{16}$	$c/l=\frac{11}{16}$	$c/l=\frac{14}{16}$
0	1	1	1	1	1	1	1
0.1	1	1	1	0.9932	0.9932	0.9932	1
0.2	1	0.9932	1	0.9864	0.9864	0.9932	1
0.3	1	0.9863	1	0.9796	0.9728	0.9864	1
0.4	1	0.9658	1	0.9728	0.9524	0.9864	1
0.5	0.9932	0.9521	0.9932	0.9524	0.9388	0.9864	0.9864
0.6	0.9932	0.9315	0.9932	0.9388	0.8980	0.9796	0.9864
0.7	0.9932	0.9041	0.9932	0.898	0.8844	0.9796	0.9864

frequency was least affected (generally) when c/l was $\frac{3}{16}$, and mostly affected at the center (actually the largest effect will be felt at the fixed ends, but, no measurements could be made at that location). The results for $c/l=\frac{1}{16}$ in a fixed beam were not available due to experimental errors. Hence for a simply supported beam, it could be inferred (from the measured data) that the fundamental frequency decreases significantly as the crack location moves towards the

Table 4
Fundamental natural frequency ratio (ω_c/ω) as a function of crack location and crack depth for a simply supported beam

a/h	$c/l=\frac{1}{16}$	$c/l=\frac{3}{16}$	$c/l=\frac{5}{16}$	$c/l=\frac{7}{16}$	$c/l=\frac{8}{16}$	$c/l=\frac{11}{16}$	$c/l=\frac{14}{16}$
0	1	1	1	1	1	1	1
0.1	1	0.9980	0.9923	0.9960	0.9940	0.9980	0.9994
0.2	1	0.9956	0.9892	0.9849	0.9970	0.9968	0.9990
0.3	1	0.9881	0.9758	0.9686	0.9530	0.9797	0.9978
0.4	0.9995	0.9781	0.9507	0.9418	0.9234	0.9617	0.9971
0.5	0.9974	0.9664	NA	0.8961	0.8724	0.9225	0.9945
0.6	0.9930	0.9371	0.8680	0.8318	0.8119	0.8546	0.9893
0.7	0.9848	0.8756	0.7896	0.7065	0.7085	0.7713	0.9829

Table 5
Second natural frequency ratio (ω_c/ω) as a function of crack location and crack depth for a simply supported beam

a/h	$c/l=\frac{1}{16}$	$c/l=\frac{3}{16}$	$c/l=\frac{5}{16}$	$c/l=\frac{7}{16}$	$c/l=\frac{8}{16}$	$c/l=\frac{11}{16}$	$c/l=\frac{14}{16}$
0	1	1	1	1	1	1	1
0.1	1	0.9962	0.9967	0.9994	0.9999	0.9979	0.9994
0.2	0.9991	0.9889	0.9903	0.9976	0.9998	0.9889	0.9975
0.3	0.9963	0.9712	0.9767	0.9952	0.9995	0.9774	0.9936
0.4	0.9817	0.9481	0.9524	0.9918	0.9995	0.9613	0.9905
0.5	0.9848	0.9232	NA	0.9861	0.9995	0.9337	0.9824
0.6	0.9714	0.8818	0.8902	0.9811	0.9990	0.8988	0.9696
0.7	0.9544	0.8175	0.8424	0.9704	0.9986	0.8693	0.9578

Table 6
Third natural frequency ratio (ω_c/ω) as a function of crack location and crack depth for a simply supported beam

a/h	$c/l=\frac{1}{16}$	$c/l=\frac{3}{16}$	$c/l=\frac{5}{16}$	$c/l=\frac{7}{16}$	$c/l=\frac{8}{16}$	$c/l=\frac{11}{16}$	$c/l=\frac{14}{16}$
0	1	1	1	1	1	1	1
0.1	1	1	1	1	1	1	1
0.2	0.9915	1	1	0.9915	0.9915	1	1
0.3	0.9915	0.9828	1	0.9829	0.9744	0.9915	1
0.4	0.9829	0.9741	1	0.9744	0.9573	0.9915	0.9914
0.5	0.9658	0.9569	NA	0.9402	0.9402	0.9915	0.9828
0.6	0.9573	0.9483	1	0.8547	0.9145	0.9915	0.9483
0.7	0.9402	0.9310	1	0.8245	0.8014	0.9915	0.9310.50

center of the crack. The highest decrease occurs for a centrally located crack, with the exception of a crack located at the supports, which could not be considered in this study.

(2) The second natural frequency was almost unaffected for a crack located at the center of a fixed beam or a simply supported beam; the reason for this zero influence was that the nodal point for the second mode was located at the center for both types of beams.

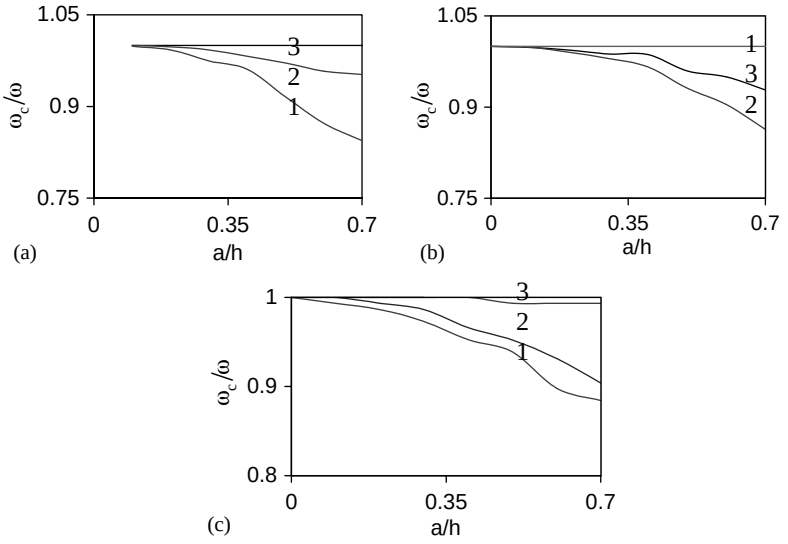

Fig. 2. Natural frequencies (of various modes) in terms of crack depth for a fixed–fixed beam for various crack location ratios c/l ($1\rightarrow\frac{8}{16}; 2\rightarrow\frac{5}{16}; 3\rightarrow\frac{3}{16}$): (a) mode 1; (b) mode 2; and (c) mode 3.

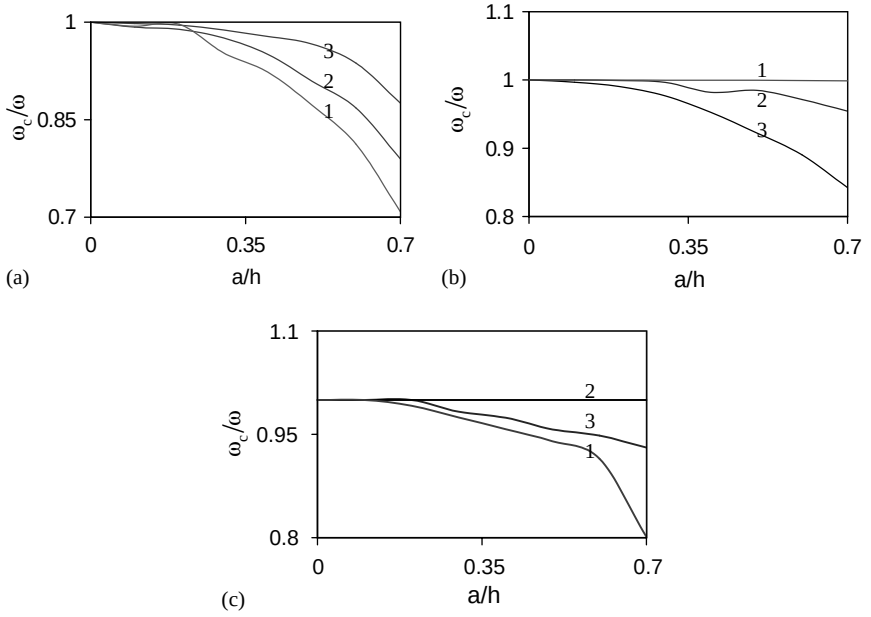

Fig. 3. Natural frequencies (of various modes) in terms of crack depth for a simply supported beam for various crack location ratios c/l ($1\rightarrow\frac{8}{16}; 2\rightarrow\frac{5}{16}; 3\rightarrow\frac{3}{16}$): (a) mode 1; (b) mode 2; and (c) mode 3.

(3) The third natural frequencies of both the fixed and the simply supported beams changed rapidly for a crack located at the center.
(4) Due to shifts in the nodal positions (as a consequence of cracking) of the second, and the third modes, the changes in the higher natural frequencies depended on how close the crack

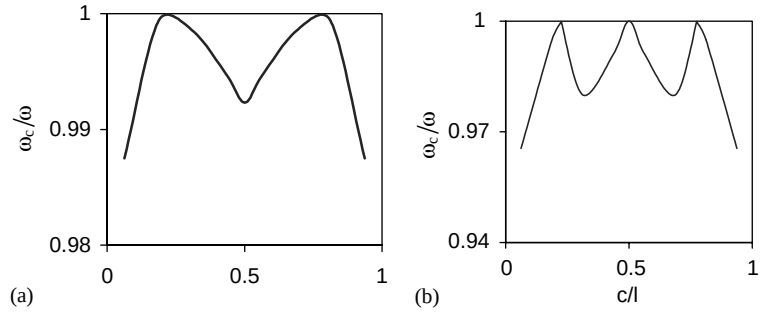

Fig. 4. Variation of the first two natural frequencies as a function of crack location for a fixed-end beam (crack depth ratio $a/h = 0.2$): (a) first natural frequency and (b) second natural frequency.

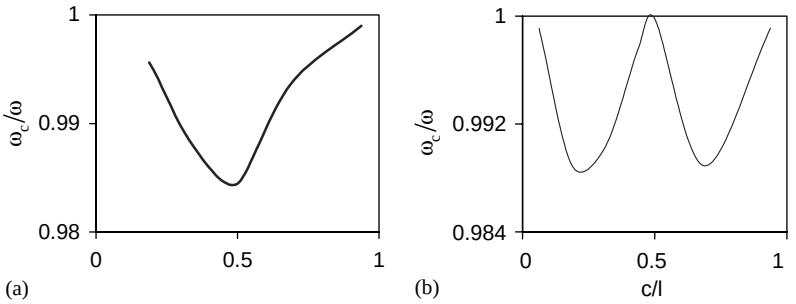

Fig. 5. Variations of the first two natural frequencies as a function of crack location for a simply supported beam (crack depth ratio $a/h = 0.2$): (a) first natural frequency and (b) second natural frequency.

location was to the mode shape nodes. Consequently, it could be observed from the Tables 2, 3, 5 and 6 that the trend of changes in the second, and the third frequencies are not monotonic, as we have in the first natural frequency.

(5) From the results obtained, it is observed, for example, that when the crack depth ratio is 0.6, the third natural frequency was comparatively much less affected than the first and second frequencies for a crack located at 203 mm ($c/l = \frac{5}{16}$) from one end of the simply supported beam. It was affected considerably for other crack locations (see Table 6). This could be explained by the fact that the decrease in frequencies is greatest for a crack located where the bending moment is greatest. It appears therefore that the change in frequencies is not only a function of crack depth, and crack location, but also of the mode number.

(6) For a few of the cases considered, the frequencies remained unchanged until a certain value of crack depth ratio was attained, after which, the frequencies decreased rapidly. For example, in the case of a simply supported beam, at a crack location of $\frac{3}{16}$ of the length of the beam, the third natural frequency was almost unchanged until a crack depth ratio of $\frac{3}{10}$ was achieved. For larger values of crack depth ratios, the frequencies decreased rapidly (see Table 6).

As stated earlier, the decrease in the fundamental natural frequency was greatest when the crack occurred at the middle point. This could be explained by the fact that the dynamic bending

moment was the largest at the middle point (where the amplitude of the first mode shape is greatest) for the first mode, thereby, resulting in a greater loss of bending stiffness due to the crack. However, the second, and third modes were less affected at this location.

From the above observations, it could be stated that knowing the crack position (prior to the crack size assessment) could result in accurate prediction of its extent in a crack identification problem if one uses only one mode. Otherwise it becomes very difficult, since the results could be misleading. To cite an example, the use of data obtained for the third mode of a simply supported beam (refer to Table 6, crack located at 203 mm; $c/l = \frac{5}{16}$) would lead to the conclusion that the beam is undamaged since no frequency changes are observed for all the crack depths considered. In general, the higher the number of modes used, the greater the degree of accuracy, and dependability of predicted results.

4.3. Changes in mode shapes

The mode shapes obtained for some of the cases considered for both the simply supported and fixed beams are shown in Figs. 6 and 7. For most of the cases considered, as the crack grows, the mode shapes undergo a highly noticeable change close to the crack location area. In some cases, as the crack grows deeper (when the crack depth was equal to or greater than 0.5), there were shifts in the position of the nodes for the second and third modes. The changes in the natural frequency, and mode shape depended on how close the crack was to nodes of mode shapes for higher modes. Thus, based on the observed changes in the natural frequencies, and mode shapes, the crack position, and crack depth can be estimated.

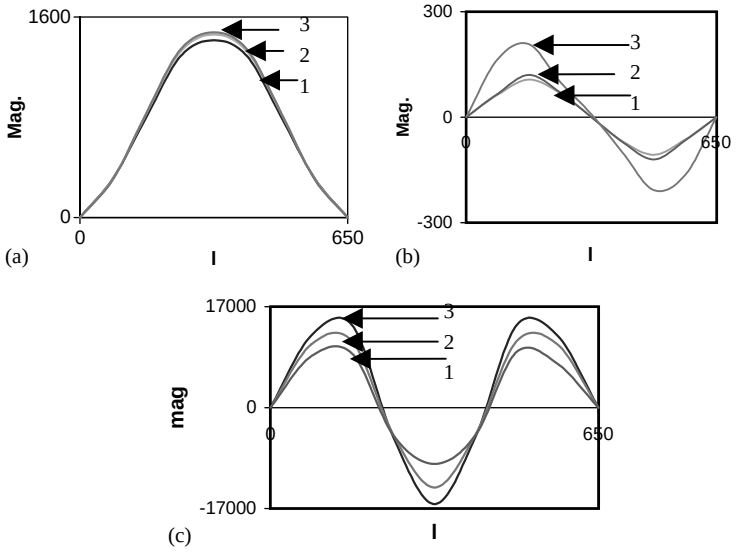

Fig. 6. Mode shapes of a fixed beam with crack location $c/l = \frac{3}{16}$ for different crack depths (1: $a/h = 0$, uncracked; 2: $a/h = 0.3$; 3: $a/h = 0.5$): (a) mode 1; (b) mode 2; and (c) mode 3.

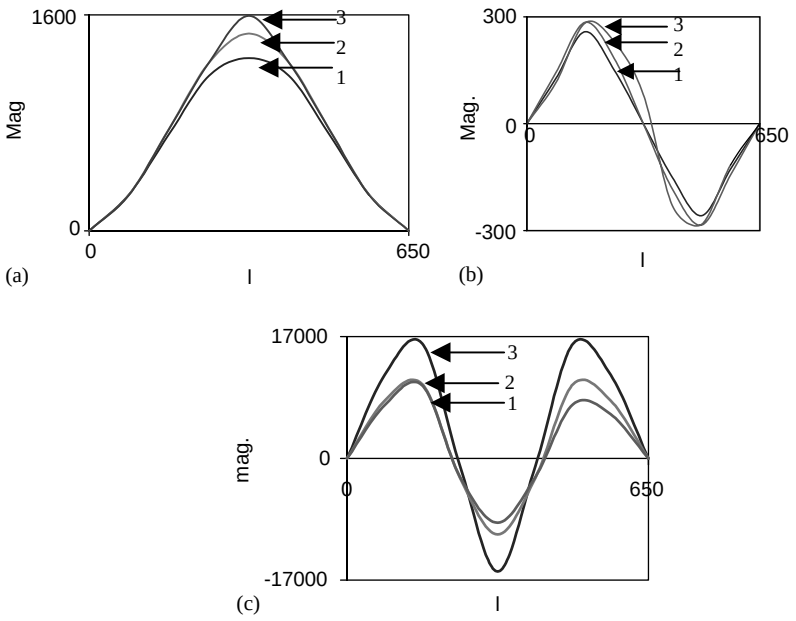

Fig. 7. Mode shapes of a fixed beam with crack location $c/l = \frac{8}{16}$ for different crack depths (1: $a/h = 0$, uncracked; 2: $a/h = 0.3$; 3: $a/h = 0.5$): (a) mode 1; (b) mode 2; and (c) mode 3.

For a crack located at the center of a fixed beam, the second mode is minimally affected for most of the crack ratios considered as shown in Fig. 7. The third mode deformations are affected to a greater extent than the first mode.

4.4. *Frequency response functions*

As stated earlier, several FRFs were obtained in these experimental investigations for a combination of different crack depths and crack locations. Due to the fact that the natural frequencies are global properties of the beams, their shifts could be observed by using the FRF measurements taken from virtually any point on the beams. The FRFs obtained (at least 21 for each of the 14 models) were too numerous to be given fully in this paper. However, some of the measured FRFs are presented in this section to illustrate the shifts that occurred in the amplitudes and frequencies for the first three modes.

Fig. 8 shows typical FRFs measured for the first three modes of vibration for different crack depth ratios, for a crack located at the center of a fixed beam. From Fig. 8(a), it could be observed that the fundamental frequency ratios show a clear downward trend (in its shifting) as the crack depth ratio increases. The amplitude of the FRF also shows a decreasing trend, as the crack grows in size. Fig. 8(b) shows that the reduction in the amplitude of the FRF, of the second mode, was similar to the first mode. The amplitude changes in mode three could be observed in Fig. 8(c). The amplitude changes observed for the third mode do not show trends similar to mode 1 for increasing crack depth but rather show an increase. The peak noted at a frequency of 1031 Hz in

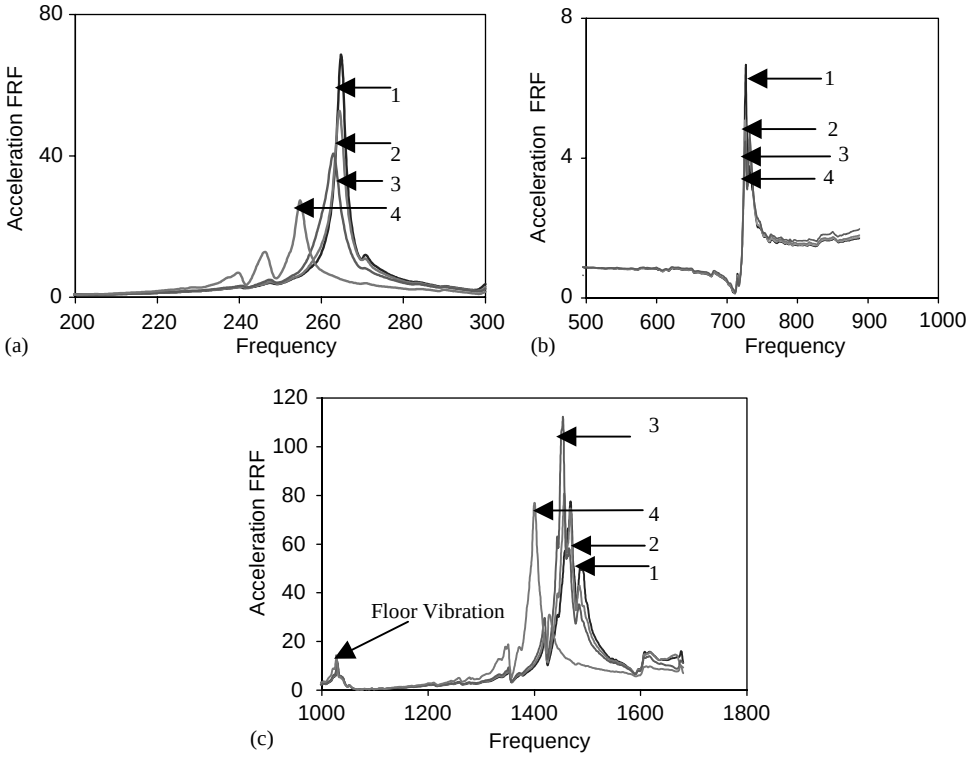

Fig. 8. Natural frequencies shifts and FRF amplitude reduction for a crack located at the center of a fixed beam for various crack depth ratios a/h—accelerometer located at $\frac{1}{4}$th the span of the beam from left (1: uncracked; 2: $a/h = 0.1$; 3: $a/h = 0.2$; 4: $a/h = 0.4$): (a) first natural frequency; (b) second natural frequency; and (c) third natural frequency.

Fig. 8 was one of the resonance peaks introduced into the measurements by floor vibration. This was detected by using the eighth accelerometer (as mentioned earlier in the paper).

Fig. 9 shows the FRFs for the first three modes of vibration in a simply supported beam for cracks located at a crack location ratio (c/l) of $\frac{5}{16}$. For a crack located at $c/l = \frac{5}{16}$, the behavior was similar to the first three modes of the fixed-end beam (with the crack located at the center).

4.5. Crack identification technique

Based on the measured frequency and amplitude changes, a method for identifying a crack location and crack depth is presented in this section.

4.5.1. Crack identification technique using changes in natural frequencies

As stated earlier, both the crack location and the crack depth influence the changes in the natural frequencies of a cracked beam. Consequently, a particular frequency could correspond to different crack locations and crack depths. This can be observed from the three-dimensional plots of the first three natural frequencies of beams with fixed and simply supported ends, shown in Figs. 10 and 11, respectively. On this basis, a contour line, which has the same normalized

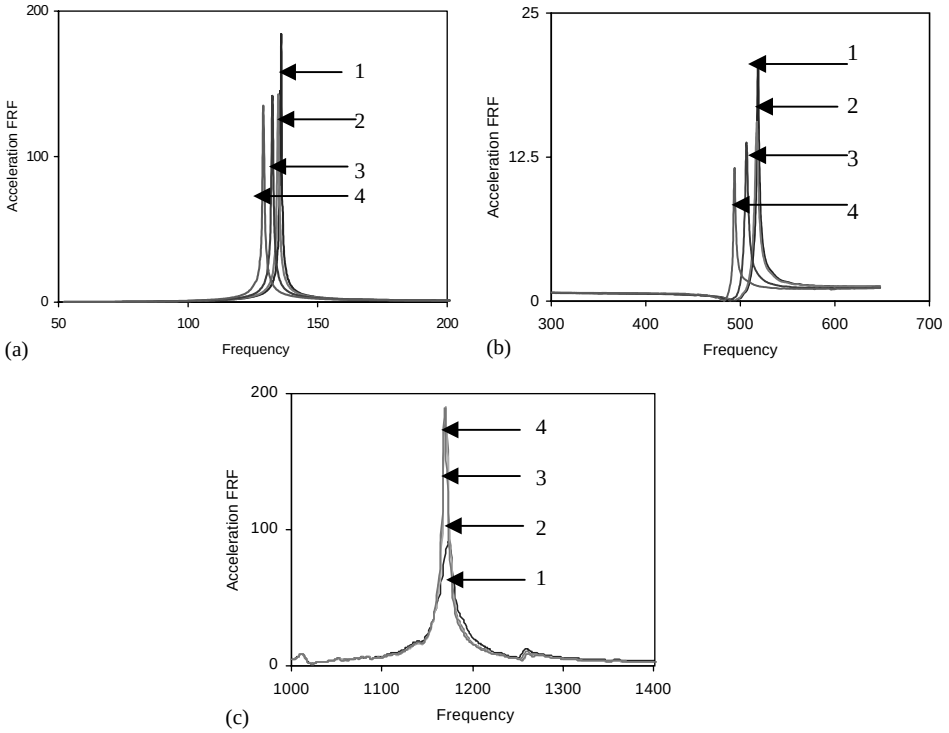

Fig. 9. Natural frequency shifts and FRF amplitudes for a crack located at a crack length ratio c/l of $\frac{5}{16}$ of a simply supported beam for various crack depth ratios a/h—accelerometer located at $\frac{1}{4}$th of the span of the beam from left (1: uncracked; 2: $a/h = 0.1$; 3: $a/h = 0.2$; 4: $a/h = 0.4$): (a) first natural frequency; (b) second natural frequency; and (c) third natural frequency.

frequency change resulting from a combination of different crack depths and crack locations (for a particular mode) could be plotted in a curve with crack location and crack depth as its axes. For illustrative purposes, the contour lines for the first and second modes of simply supported and fixed-end beams are shown in Figs. 12 and 13, respectively. The normalized frequencies shown in the figures are 0.9900 (a decrease of 1% in frequency) for the first mode and 0.9800 (a decrease of 2% in frequency) for the second mode (these values were obtained by linear interpolation from adjacent values).

To identify the presence of one or more cracks in the beam, an essential step is to measure a sufficient number of natural frequencies of the beam, and then use the technique explained in this section to estimate the crack location(s), and depth(s). The number of cracks on the beam determines the required number of frequencies and mode shapes to be measured or computed. Measuring the first three natural frequencies will be sufficient to determine the crack location, and the crack depth for a beam with a single crack. For a beam with a single crack with unknown parameters, the following steps are required to predict the crack location, and depth, namely, (1) measurements of the first three natural frequencies; (2) normalization of the measured frequencies; (3) plotting of contour lines from different modes on the same axes; and (4) location

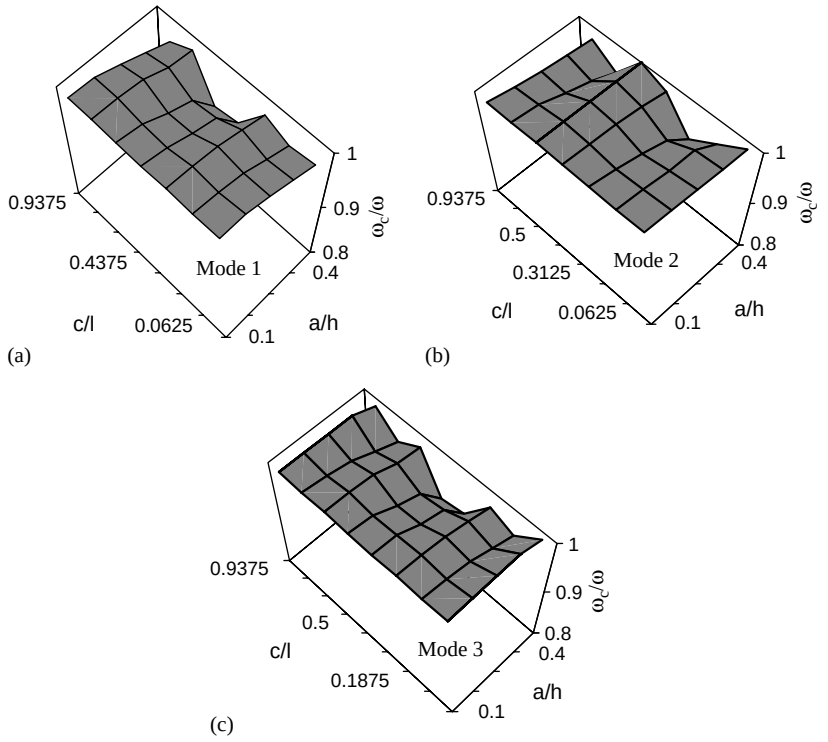

Fig. 10. Three-dimensional plots of frequency ratio versus crack location, and crack depth for a fixed–fixed beam: (a) mode 1; (b) mode 2; and (c) mode 3.

of the point(s) of intersection of the different contour lines. The point(s) of intersection, common to all the three modes, indicate(s) the crack location(s), and crack depth(s). This intersection becomes unique due to the fact that any normalized crack frequency can be represented by a governing equation that is dependent on normalized crack depth (a/h), normalized crack location (c/l) and mode number. Therefore a minimum of three curves is required to identify the two unknown parameters of normalized crack location and crack depth.

From Tables 1–3 (beam with a fixed end), it is observed that for a crack depth ratio of 0.1 located at a distance of $\frac{7}{16}$ of the length of the beam, the normalized frequencies are 0.9977 (i.e., a decrease of 0.23% in frequency) for the first mode, 0.9989 for the second mode and 0.9932 for the third mode. The contour lines with the values of 0.9977, 0.9989 and 0.9932 were retrieved (by linear interpolation) from the first three modes (see Fig. 10) and plotted on the same axes as shown in Fig. 14. From the figure it could be observed that there are four intersection points in the contour lines of the first and the second modes. Consequently the contour of the third mode is used to identify the crack location ($c/l = \frac{7}{16}$) and the crack depth ratio ($a/h = 0.1$), uniquely. The three contour lines gave just one common point of intersection, which indicates the crack location and the crack depth. As mentioned earlier, the contour lines obtained are not perfectly symmetrical due to the limited number of measuring points considered during the experimentation. Similar procedures were applied to a simply supported beam (with a crack depth of $a/h =$

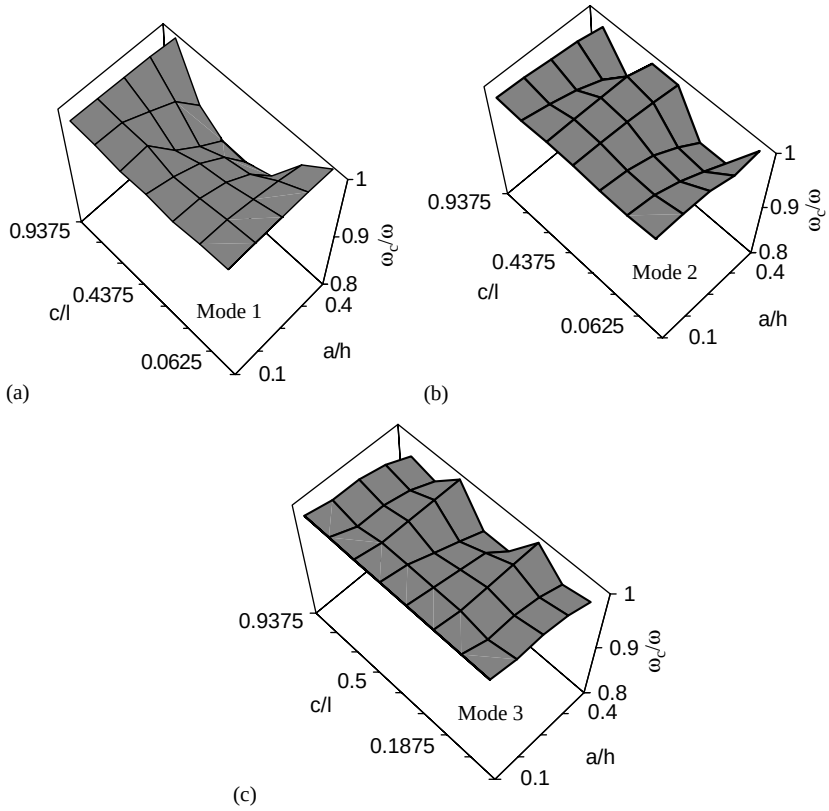

Fig. 11. Three-dimensional plots of frequency ratio versus crack location, and crack depth for a simply supported beam: (a) mode 1; (b) mode 2; and (c) mode 3.

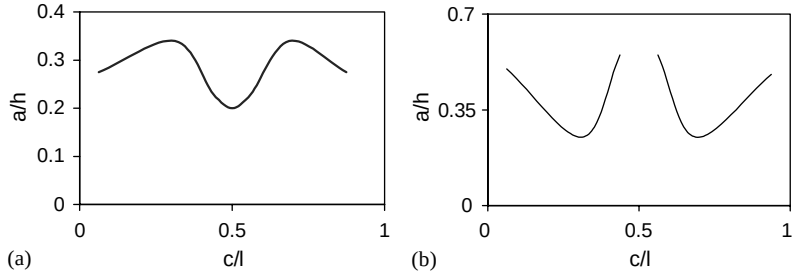

Fig. 12. Frequency contour plots for a simply supported beam: (a) mode 1 and (b) mode 2.

0.3 and located at $c/l = \frac{3}{16}$) in which the normalized frequencies were 0.9881, 0.9712 and 0.9828 for the first three modes (see Tables 4–6), respectively. The contour lines obtained (see Fig. 11), which indicate the crack location ($c/l = \frac{3}{16}$) and the crack depth ($a/h = 0.3$), are shown in Fig. 15.

This technique appears to be good in identifying cracks in beams, because a crack will definitely belong to a contour line for each mode, and measuring the lowest three natural frequencies in a beam is not a difficult task as long as measuring errors are reduced to a minimum or eliminated.

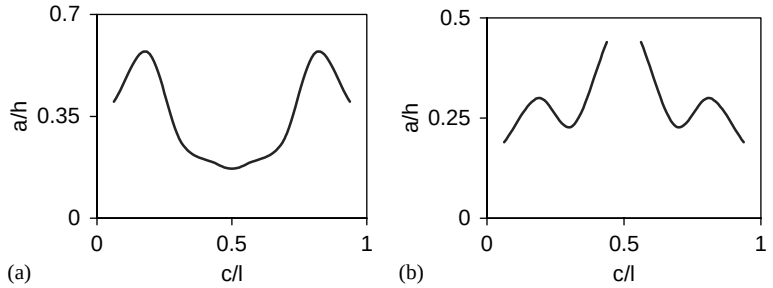

Fig 13. Frequency contour plots for a fixed–fixed beam: (a) mode 1; and (b) mode 2.

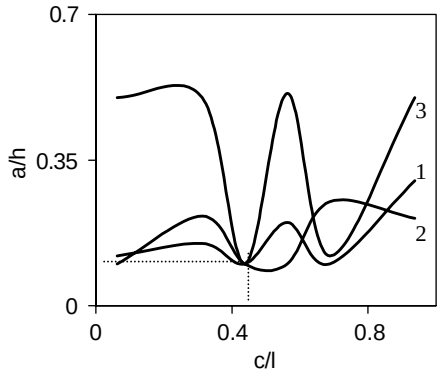

Fig. 14. Crack identification technique by using frequency contours of the first three modes of a fixed beam (1: mode 1, normalized frequency (0.9977); 2: mode 2, normalized frequency (0.9989); and 3: mode 3, normalized frequency (0.9932)).

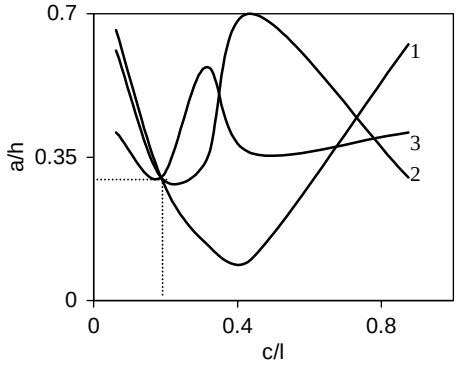

Fig. 15. Crack identification technique using frequency contours of first three modes in a simply supported beam (1: mode 1, normalized frequency (0.9881); 2: mode 2, normalized frequency (0.9712); 3: mode 3, normalized frequency (0.9828)).

In a situation whereby the crack location coincides with a vibration node, the contour line tends to disappear, and no intersections can be obtained. In such a case, higher modes may have to be obtained to predict the location, and the depth of the crack. Beams containing two cracks have been considered by Yang et al. [18], and as long as the interaction between adjacent cracks are marginal (less than 5%), the above approach can be used to detect multiple cracks. There are several parameters that need to be investigated in such studies such as the number of cracks, crack interaction effects, interaction between axial and flexural vibrations, rotation and settlement of the supporting boundaries, etc. These parameters may be investigated in the future by the authors.

4.5.2. Crack identification technique using changes in amplitudes

In Section 4.4, it was noted that a crack in a beam affects the amplitudes of the measured FRFs. Based on the changes of amplitudes of the FRFs, a method similar to that discussed in the preceding section could be developed for identifying the crack location and crack depth. Figs. 16 and 17 show, respectively, the three-dimensional plots of the changes in the normalized amplitudes (H_c/H_u, ratio of the amplitudes of the FRF of the cracked beam to that of the uncracked beam) of the first three modes of fixed–fixed and simply supported beams versus crack location and crack depth ratios (for the third accelerometer located at a distance of $\frac{3}{8}$ of the length

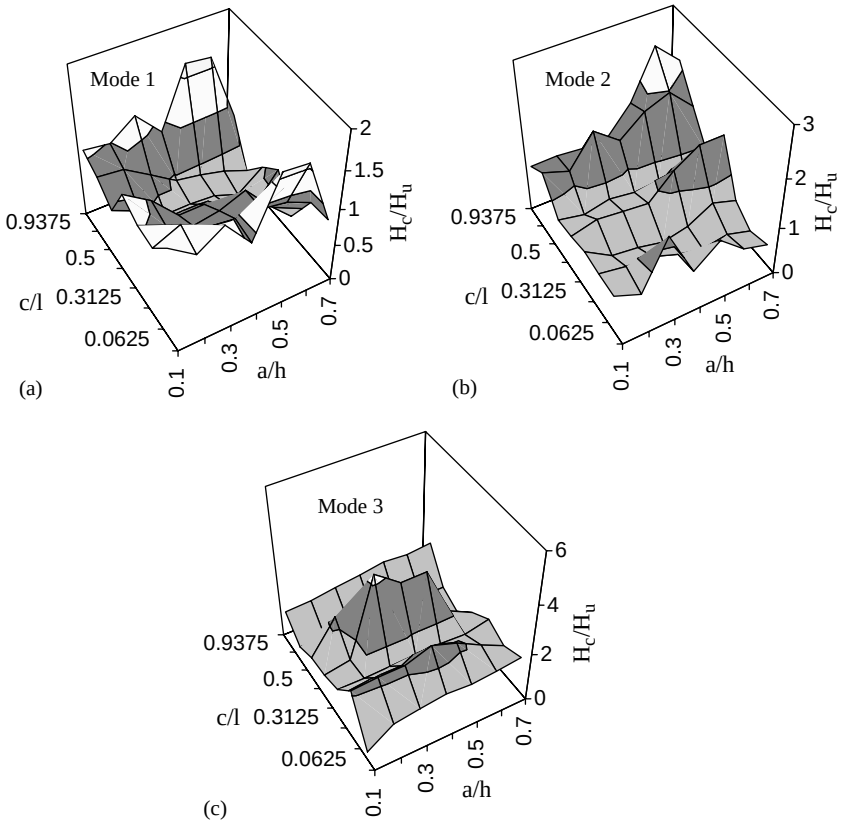

Fig. 16. Three-dimensional plots of amplitude ratio versus crack location, and crack depth for a fixed–fixed beam. Accelerometer located at $\frac{3}{8}$th the span of the beam from left: (a) mode 1; (b) mode 2; and (c) mode 3.

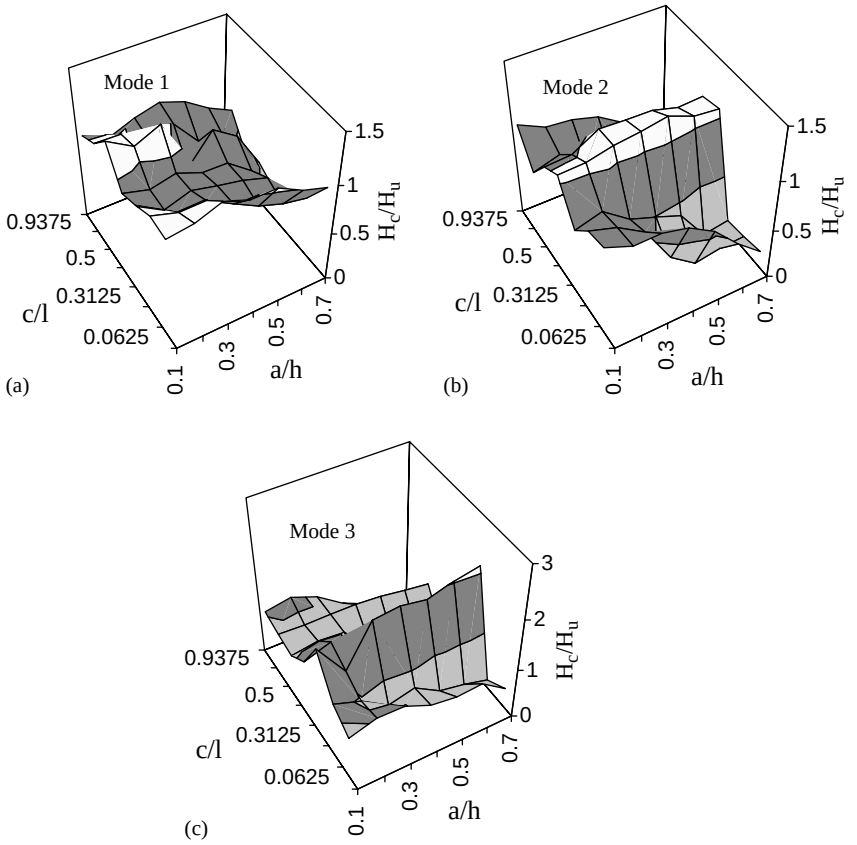

Fig. 17. Three-dimensional plots of amplitude ratio versus crack location, and crack depth for a simply supported beam—accelerometer located at $\frac{3}{8}$th the span of the beam from left: (a) mode 1; (b) mode 2; and (c) mode 3.

of the beam from one of its ends). It could be observed from the three-dimensional plots that both crack location and crack depths affect the changes in amplitudes. Consequently, a contour line which has the same normalized amplitude changes resulting in a combination of different crack location and crack depths could be plotted as a curve with crack location and crack depth as its axes (similar to the one discussed earlier in the preceding section).

The various steps enumerated in the preceding section for identifying crack location and crack depth in a beam with a crack (using frequencies) can also be applied to amplitude changes of the tested beam. Fig. 18 shows the application of this technique to identify a crack in a fixed beam for a crack depth of 0.1 located at a distance of $\frac{8}{16}$ of the length of the beam. The normalized amplitudes for the first three modes are 0.7121, 0.7505, and 0.9943, respectively. The contour lines with the values 0.7121, 0.7505, and 0.9943 were retrieved (by linear interpolation) from the first three modal responses and plotted on the same axes in Fig. 18. It could be observed that there are two intersection points of the contour lines of the first and second modes. Hence, in a manner similar to the preceding section, the unique values of the crack location and crack depths were obtained by plotting the contour line of the third mode. Similar procedures were applied to a

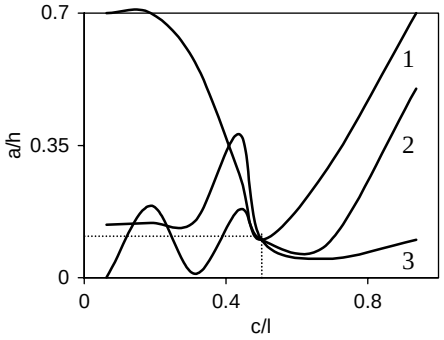

Fig. 18. Crack identification technique by using amplitude contours of the first three modes of a fixed beam—accelerometer located at $\frac{3}{8}$th the span of the beam from left (1: mode 1, normalized amplitude (0.7121); 2: mode 2, normalized amplitude (0.7505); and 3: mode 3, normalized amplitude (0.9943))—identified crack ($c/l = \frac{8}{16}; a/h = 0.1$).

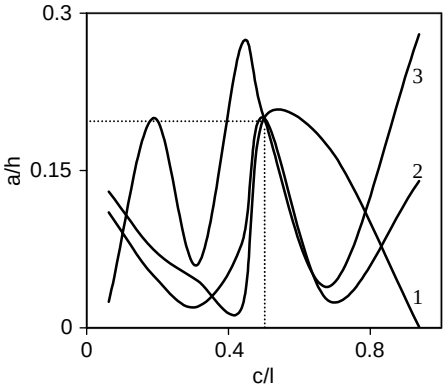

Fig. 19. Crack identification technique by using amplitude contours of the first three modes of a simply supported beam—accelerometer located at $\frac{3}{8}$th the span of the beam from left (1: mode 1, normalized amplitude (0.9998); 2: mode 2, normalized amplitude (0.9613); 3: mode 3, normalized amplitude (0.9575))—identified crack ($c/l = \frac{8}{16}; a/h = 0.2$).

simply supported beam (with a crack depth ratio of 0.2 and located at $c/l = \frac{8}{16}$), and the contour lines obtained are shown in Fig. 19 for the first three modes.

5. Comparison of the experimental and theoretical results

Theoretical analyses of the cracked beam were carried out by Yang et al. [18]. In this paper, an energy-based numerical model was developed to investigate the influence of cracks on the structural dynamic characteristics during the vibration of a beam. Upon the determination of strain energy in the cracked beam, the equivalent bending stiffness over the beam length was computed. The cracked beam was then taken as a continuous system with varying moment of

Table 7
Comparison of the experimental and theoretical natural frequencies of fixed–fixed beams for a centrally located crack ($c/l = 0.5$) having different crack depth ratios (a/h)

Crack depth ratio	First mode			Second mode			Third mode		
	Exp.[a]	TR.[b]	(Rel. Diff.)[c] (%)	Exp.	TR.	(Rel. diff.) (%)	Exp.	TR.	(Rel. diff.) (%)
0.1	0.9985	0.9987	0.020	1.0000	1.0000	0.000	0.9932	0.9938	0.060
0.2	0.9923	0.9935	0.120	1.0000	1.0000	0.000	0.9864	0.9870	0.060
0.3	0.9746	0.9750	0.010	1.0000	1.0000	0.000	0.9728	0.9740	0.120
0.4	0.9608	0.9614	0.006	1.0000	0.9998	0.020	0.9524	0.9532	0.080
0.5	0.9159	0.9200	0.440	1.0000	0.9992	0.080	0.9388	0.9400	0.130

[a] Experimental values.
[b] Theoretical values.
[c] Relative difference (absolute relative difference expressed as a percentage).

Table 8
Comparison of the experimental and theoretical natural frequencies of simply supported beams for a centrally located crack ($c/l = 0.5$) having different crack depth ratios (a/h)

Crack depth ratio	First mode			Second mode			Third mode		
	Exp.	TR.	(Rel. diff.) (%)	Exp.	TR.	(Rel. diff.) (%)	Exp.	TR.	(Rel. diff.) (%)
0.1	0.9940	0.9946	0.060	0.9999	1.0000	0.010	1.0000	1.0000	0.000
0.2	0.9770	0.9780	0.100	0.9998	0.9997	0.010	0.9915	0.9920	0.050
0.3	0.9530	0.9536	0.060	0.9995	0.9993	0.020	0.9744	0.9750	0.060
0.4	0.9234	0.9240	0.060	0.9995	0.9990	0.050	0.9573	0.9580	0.070
0.5	0.8724	0.8730	0.070	0.9995	0.9988	0.070	09402	0.9410	0.080

See Table 7.

inertia, and equations of transverse vibration were obtained for a rectangular beam containing one or two cracks. Galerkin's method was utilized to solve for the frequencies and vibration modes. The crack depth ratio considered was from 0.1 to 0.5, and for each crack depth ratio, the natural frequency ratio was calculated.

The natural frequency ratios presented in Yang et al.'s paper [18] were for a crack located at the center of the beam for both the simply supported and fixed beams. Tables 7 and 8 show the results obtained theoretically and experimentally. The results compare very well.

6. Conclusions

Detailed experimental investigations of the effects of cracks on the first three modes of vibrating beams (simply supported and fixed beams) have been presented in this paper. The vibration behavior of the beams is shown to be very sensitive to the crack location, crack depth and mode number. A simple method for predicting the location(s) and depth(s) of the crack(s) based on changes in the natural frequencies and amplitudes of the FRFs of the beam is also presented, and

discussed. This procedure becomes feasible due to the fact that under robust test and measurement conditions, the measured parameters of frequencies and response amplitudes are unique values, which will remain the same (within a tolerance level), wherever similar beams are tested and responses measured. Since the frequencies and amplitudes depend on the crack depth and location, these values can be uniquely determined by the solution of a function having solutions one order higher (in this case, three) than the number of unknowns (in this case, two, namely crack depth and location) to be determined. This is the reason for the requirement of three modes. If there were more parameters that influence the response (besides the crack depth and location), then one will require more modes to identify the unknown crack depth and crack location.

References

[1] M.H. Richardson, Detection of damage in structures from changes in their dynamic (modal) properties, A Survey, NUREG/CR-1431, US, Nuclear Regulatory Commission, Washington, DC, 1980.
[2] S.W. Doebling, C.R. Farrar, M.B. Prime, P.W. Shevitz, Damage identification, Health monitoring of structural, and mechanical systems from changes in their vibration characteristics, A Literature Review, Los Alamos National Laboratory, Los Alamos, New Mexico, 1996, 100pp.
[3] P. Cawley, R.D. Adams, The location of defects in structures from measurement of natural frequencies, Journal of Strain Analysis 14 (2) (1979) 49–57.
[4] J.M.M. Silva, A.J.M.A. Gomes, Experimental dynamic analysis of cracked free–free beams, Journal of Experimental Mechanics 30 (1) (1994) 20–25.
[5] F. Ju, M. Mimovich, Modal frequency method in diagnosis of fracture damage in structures, Proceedings of the Fourth International Modal Analysis Conference, Los Angeles, CA, 1986, pp. 1423–1429.
[6] C.H.J. Fox, The location of defects in structures: a comparison of the use of natural frequencies and mode shape data, Proceedings of the 10th International Modal Analysis Conference, San Diego, CA, 1992, pp. 522–528.
[7] M.R. Chowdhury, M. Ramirez, A comparison of the modal responses for defective versus non-defective concrete test beams, Proceedings of the 10th International Modal Analysis Conference, San Diego, CA, 1992, pp. 508–515.
[8] M.B. Prime, D.W. Shevitz, Linear and nonlinear methods for detecting cracks in beams, Proceedings of the 14th International Modal Analysis Conference, Honolulu, HI, 1996, pp. 1437–1443.
[9] N. Stubbs, Global nondestructive evaluation of solids, The International Journal of Analytical and Experimental Modal Analysis 5 (2) (1990) 67–79.
[10] T.G. Chondros, A.D. Dimarogonas, Identification of cracks in welded joints of complex structures, Journal of Sound and Vibration 69 (4) (1980) 531–538.
[11] T.G. Chondros, A.D. Dimarogonas, Dynamic sensitivity of structures to cracks, Journal of Vibration, Acoustics, Stress and Reliability in Design 111 (1989) 251–256.
[12] T.G. Chondros, A.D. Dimarogonas, Vibration of a cracked cantilever beam, Journal of Vibration and Acoustics, Transactions of the American Society of Mechanical Engineers 120 (1998) 742–746.
[13] S. Christides, A.D.S. Barr, One-dimensional theory of cracked Bernoulli–Euler beams, International Journal of Mechanical Sciences 26 (11/12) (1984) 639–648.
[14] D.R. Perchard, A.S.J. Swamidas, Crack detection in slender cantilever plates using modal analysis, Proceedings of the 12th International Modal Analysis Conference, Honolulu, HI, 1994, pp. 1769–1777. (Also see the M. Eng. Thesis of D.R. Perchard on Crack Detection in slender cantilever plates using modal analysis, Memorial University of Newfoundland, St. John's, Canada, May 1993, 236pp.)
[15] A. Budipriyanto, A.S.J. Swamidas, Experimental and analytical verification of modal behavior of uncraked/cracked plates in air and water, Proceedings of the 12th International Modal Analysis Conference, San Diego, CA, 1994, pp. 745–752.

[16] Y. Chen, A.S.J. Swamidas, Modal parameters identification for fatigue crack detection in T-plate joints, Proceedings of the 14th International Modal Analysis Conference, Honolulu, HI, pp. 112–118. (Also see the Ph.D. Thesis of Y. Chen on Crack detection in plated T-joints through vibration techniques, submitted to Memorial University, St. John's, NF, Canada, June 1996, 160pp.)
[17] R.J. Allemang, Vibrations: Experimental Modal Analysis, Structural Dynamics laboratory, Department of Mechanical, Industrial, and Nuclear Engineering, University of Cincinnati, Ohio, USA, 1990.
[18] X.F. Yang, A.S.J. Swamidas, R. Seshadri, Crack identification in beams using energy method, Journal of Sound and Vibration 244 (2) (2001) 339–357.